IEEE Access
Multidisciplinary ⋮ Rapid Review ⋮ Open Access Journal

Received August 6, 2021, accepted September 6, 2021, date of publication September 10, 2021,
date of current version September 17, 2021.

Digital Object Identifier 10.1109/ACCESS.2021.3112036

Simulating Immunization Campaigns and Vaccine Protection Against COVID-19 Pandemic in Brazil

FABIO AMARAL[1], WALLACE CASACA[2], CASSIO M. OISHI[1], AND JOSÉ A. CUMINATO[3]
[1]Faculty of Science and Technology, São Paulo State University (UNESP), Presidente Prudente 19060-900, Brazil
[2]Department of Energy Engineering, São Paulo State University (UNESP), Rosana 19273-000, Brazil
[3]Institute of Mathematics and Computer Sciences, University of São Paulo (USP), São Carlos 13566-590, Brazil

Corresponding author: Wallace Casaca (wallace.casaca@unesp.br)

This work was supported in part by São Paulo Research Foundation (FAPESP) under Grant 2013/07375-0 and Grant 2021/03328-3, in part by the National Council for Scientific and Technological Development (CNPq) under Grant 305383/2019-1, in part by the Coordination for the Improvement of Higher Education Personnel (CAPES) under Grant 88882.441642/2019-01, and in part by Pro-Reitoria de Pos-Graduacao (UNESP).

ABSTRACT The vaccine roll-out has currently established a new trend in the fight against COVID-19. In many countries, as vaccination cover rises, the economic and social disruptions are being progressively reduced, bringing more confidence and hope to the population. However, a crucial debate is related to fair access to vaccines, which would lead to stepping up the pace of vaccination in developing countries. Another important issue is how immunization has influenced the control of the infection, deaths, and transmissibility of the new coronavirus in these countries. In this work, we investigate the effects of the rate of vaccination on the COVID-19 epidemic curves, by employing a new data-driven methodology, formulated on the basis of a modified Susceptible-Infected-Recovered model and Machine Learning designs. The data-driven methodology is applied to assess the influence of the vaccines administered in Brazil on the fight against the virus. The impacts of vaccine efficacy and immunization speed are also investigated in our study. Finally, we have found that the use of anti-SARS-CoV-2 vaccines with a low/moderate efficacy can be offset by immunizing a larger proportion of the population more quickly.

INDEX TERMS COVID-19, data-driven, SIR, vaccination, artificial intelligence.

I. INTRODUCTION

Massive vaccination campaigns are one of the most effective strategies against the COVID-19 disease. Under this premise, many countries have dedicated a considerable amount of effort in negotiating and administering different types of COVID-19 vaccines such as Pfizer/BioNTech, Oxford/AstraZeneca and CoronaVac/Sinovac in order to control the spread of new coronavirus. As a result, the nations that implemented mass vaccination early have seen a significant reduction of their SARS-CoV-2 cases and deaths, as for instance, Israel and the UK [1]–[3]. However, due to limitations on the capacity of vaccine production and the global fluctuation in its distribution, it is well-known that several countries around the world have faced enormous challenges in trying to cope with new waves of COVID-19. This is the case experienced by Brazil, a developing country that has suffered from delays in negotiating early deals with pharmaceutical companies [4] and due to the high social inequality present in the country [5]. As a consequence, the total number of new cases and deaths significantly increased in 2021, surpassing the worst scenario seen in the previous year [1].

Brazil is drawing the attention of the international community because of the rapid increase of new cases, hospitalizations and deaths so that its health system is teetering on the brink of collapse [6]. Variant P.1, which emerged at the Brazilian Amazon region, has a higher rate of transmission [7], taking the country to the worst moment of the pandemic. Also, as previously pointed out, the country has strongly been affected by the shortage of COVID-19 vaccines, so that knowing the number of doses administered per day, forecasting the number of new cases and the transmissibility levels for the months ahead can significantly contribute to the Brazilian authorities' efforts in containing the advance of the virus.

In order to carry out such a complete assessment of vaccination in Brazil, in this paper we propose a new

The associate editor coordinating the review of this manuscript and approving it for publication was Derek Abbott.

data-driven approach, whose parameters are learned from individual regressors, to model the vaccination dynamics under a two-dose regime. Unlike recent studies [8], [9] concerning vaccination in Brazil, our methodology applies Artificial Intelligence tools to predict the parameters used in a hybrid compartmental model, since most of these parameters present a transient behavior, as discussed in our recently published work [10]. As shown by the experiments, this methodology successfully captures the trend in the epidemiological curves for well-behaved data such as that of Israel, as well as for particular scenarios wherein the data is ill-conditioned, as it is the case in Brazil. We also assess the outcome from the CoronaVac/Sinovac vaccination of the adult population of Serrana's town experiment, in São Paulo State – Brazil, which is another important contribution of this work. It is worth mentioning that recently, Serrana became the world's first fully vaccinated population in consequence of the *Project S* [11], a Brazilian study conducted by *Instituto Butantan* [12] to shed light on important issues regarding mass vaccination of a population with two-dose shots of the Sinovac vaccine. Finally, this work can be extended further to investigate COVID-19 vaccine mixing, i.e., the proposed methodology allows for numerically exploring the recent idea of mix-and-match vaccination strategies [13], [14].

II. RELATED WORK

A financially inexpensive yet effective way to measure the success of vaccination from a dynamical point-of-view is by applying the classical Susceptible-Infected-Recovered (SIR) model. In fact, additional sets of Ordinary Differential Equations (ODE) can be included as part of the full SIR formulation to model the number of vaccinated individuals and their roles in the resulting dynamical system. This is the strategy adopted by many researchers, to simulate and understand the impacts of previous pandemics. For instance, Alexander *et al.* [15] investigated the spread of influenza from the so-called Susceptible-Vaccinated-Infected-Recovered-Susceptible (SVIRS) model, while Counotte *et al.* [16] studied the epidemics of Zika virus, by rearranging the SIR model to account for vaccination. Other interesting mathematical advances on SIR-based models with vaccination were also presented by Sun and Hsieh [17], Sinha *et al.* [18], and Mathur and Narayan [19].

Most recently, specific SIR-type models with vaccination compartments have been applied for dealing with the COVID-19 pandemic. The so-called SEIRD model was employed by Roy *et al.* [20] to investigate the best vaccine allocation strategy in the New York State, while Fudolig and Howard [21] introduced a multi-strain version of the SIR model to study some variations in the reproduction number of the disease. Based on the advance of the SARS-CoV-2 vaccines, Saad-Roy *et al.* [22] presented a very robust investigation concerning the single or double doses of immunizers, including the analysis of different scenarios in terms of transmission and vaccine immunity. Similarly, Harizi *et al.* [23] applied a compartmental model to investigate the dynamical behavior of COVID-19 spreading in Canada under various daily vaccination rates and vaccine efficacies. An alternative SIR-type model covering impulsive vaccination strategies has been discussed by Etxeberria-Etxaniz *et al.* [24], while the mass vaccination in Greece was analyzed by Rachaniotis *et al.* [25]. The vaccination was also considered as part of a feedback immunization control rule in the model studied by De la Sen *et al.* [26], while Mak *et al.* [27] assumed a two-dose vaccine model to explore vaccine rollout policies.

Another effective manner to assess and forecast the number of cases and deaths by COVID-19 is by applying deep learning, such as Artificial Neural Networks (ANN). Most recently, popular deep learning architectures like Recursive Neural Networks [28]–[32] and Convolutional Neural Networks [33], [34] have been successfully used to forecast COVID-19 time-series without the inclusion of compartmental models of infections dynamics [35]. However, concerning the vaccination data, the fresh literature on purely ANN-based methods is very scarce [36]. Indeed, many important issues are still open and deserve a deeper investigation, for example, the impact of COVID-19 vaccine efficacy on epidemic curves, the effect of vaccination rate according to the number of doses administered per day, the influence of not-fully vaccinated people in the dynamics of the virus spread, etc. In addition, the possibility of learning unknown parameters only from the raw data of infected, recovered, deaths, and vaccinated is an important trait of our unified approach that is not present in purely ANN-based methods. Indeed, our methodology does not require any prior knowledge of specific epidemiological data such as, for example, the transmission rate, to generate the forecasts and approximations for the model's parameters.

Therefore, aiming at addressing some of the issues raised above, in this work we propose a hybrid compartmental model based on a Susceptible-Vaccinated-Infected-Recovered-Deceased (SVIRD) formulation that combines vaccination dynamics with an effective ANN-based design for parameter estimation. Unlike classical deep learning methods which usually learn the time-series of cases and deaths, our approach learns the unknown functions of the epidemiological model while still allowing for constructing different vaccination scenarios by just redefining new control parameters such as vaccine efficacy and immunization speed.

III. MATERIALS AND METHODS

In this section, we introduce our data-driven SVIRD-based approach, quality metrics, and the data collection used to run the experiments.

A. A SVIRD-BASED MODEL INTEGRATING VACCINATION DYNAMICS AND PARAMETER LEARNING

Motivated by the SIR-based framework recently published in [10], we formulate and solve the following system of ODEs

with vaccination dynamics:

$$
\begin{aligned}
\frac{dS}{dt} &= -\nu_1 S - \beta(t) I S, \\
\frac{d\bar{V}_1}{dt} &= \nu_1 S - \beta(t) I \bar{V}_1 - \alpha_1 \bar{V}_1, \\
\frac{dV_1}{dt} &= \alpha_1 \bar{V}_1 - \beta(t) I V_1 (1-\theta_1) - \nu_2 V_1, \\
\frac{d\bar{V}_2}{dt} &= \nu_2 V_1 - \beta(t) I \bar{V}_2 (1-\theta_1) - \alpha_2 \bar{V}_2, \\
\frac{dV_2}{dt} &= \alpha_2 \bar{V}_2 - \beta(t) I V_2 (1-\theta_2), \\
\frac{dI_s}{dt} &= \beta(t) I S - (\gamma_d + \gamma_r) I_s, \\
\frac{dI_{v,1}}{dt} &= \beta(t) I (V_1(1-\theta_1) + \bar{V}_1) - \gamma_r I_{v,1}, \\
\frac{dI_{v,2}}{dt} &= \beta(t) I (V_2(1-\theta_2) + \bar{V}_2(1-\theta_1)) - \gamma_r I_{v,2}, \\
\frac{dR_s}{dt} &= \gamma_r I_s - \nu_1 R_s, \\
\frac{dR_{v,1}}{dt} &= \gamma_r I_{v,1} + \nu_1 R_s - \nu_2 R_{v,1}, \\
\frac{dR_{v,2}}{dt} &= \nu_2 R_{v,1} + \gamma_r I_{v,2}, \\
\frac{dD}{dt} &= \gamma_d I_s.
\end{aligned} \tag{1}
$$

Due to the data-driven capability for parameter fitting, the model splits the population of infected and recovered into vaccinated and non-vaccinated so that we can track the vaccinated population over time.

An illustrative representation of the mathematical model can be seen in Figure 1. Susceptible individuals are represented by S, while $\bar{V}_1$ and $\bar{V}_2$ account for the vaccinated populations that received the first and second doses, respectively, but are not yet fully immunized due to the time necessary for getting a definitive protection from vaccination. Since an individual can be infected after receiving the first dose, we have denoted this group by $I_{v,1}$. Similarly, $I_{v,2}$ represents the group of individuals vaccinated with the second dose. Moreover, in the mathematical model, $I = I_s + I_{v,1} + I_{v,2}$ gives the infected individuals, where I_s accounts for the non-vaccinated individuals. After the vaccine has taken effect, vaccinated individuals are moved to V_1 and V_2 (subscript 1 for the first dose, and 2 for the second shot). Finally, $R_{v,1}$ and $R_{v,2}$ are the recovered individuals that have been vaccinated with doses 1 and 2, respectively, while D denotes the total of deaths. Here, we assume that the vaccine has complete effectiveness in severe cases, which means that deaths come from non-vaccinated individuals. For a list of parameters and variables, see Table 1.

In our approach, the Livermore Solver for ODEs with Automatic Method Switching (LSODA) was employed for numerically solving the mathematical model (1).

Below, we provide the main steps of our computational methodology, including the redesign of the learning pipeline previously presented in [10] to account for vaccination data.

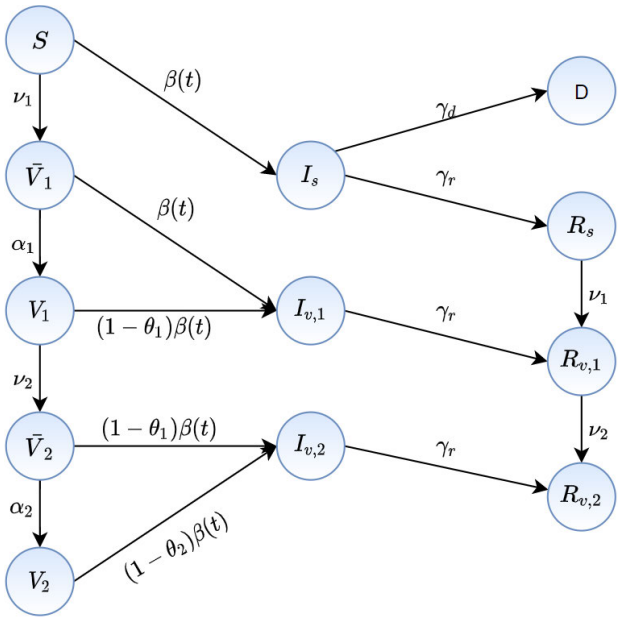

FIGURE 1. Representation of the SVIRD-based model.

TABLE 1. Basic notation.

Notation	Description
$S(t)$	Number of susceptible at time t
$I_s(t)$	Number of infected from susceptible subgroup at time t
$I_{v,j}(t)$	Number of infected from subgroup V_j, $j = 1, 2$ at time t
$I(t)$	Sum of all subgroups I_j at time t
$R_j(t)$	Number of recovered from subgroup $j = s, v_1, v_2$ at time t
$R(t)$	Sum of all subgroups R_j at time t
$D(t)$	Number of deaths at time t
$\bar{V}_i(t)$	Number of vaccinated but not yet immunized at time t, i = 1,2 doses
$V_i(t)$	Number of immunized at time t, i = 1,2 doses
$\beta(t)$	Transient transmission rate
$\beta_{\text{net}}(t)$	Prediction for the transmission rate at time t
γ_r	Rate of recovered
γ_d	Rate of lethality
ν_1 and ν_2	First and second dose vaccination rates, respectively
θ_1 and θ_2	First and second dose efficacies, respectively
α_i	Time delay for vaccine dose effectiveness, i = 1,2 doses
$R_t(t)$	Time-dependent effective reproduction number
M	Pre-specified training period
p	Desirable forecast period
Y_i and $\tilde{Y}_i$	Real and predicted daily values w.r.t. a given target variable

1) ARCHITECTURE OF THE ARTIFICIAL NEURAL NETWORK

In order to learn the transient behavior of the epidemiological parameters, we employ an Artificial Neural Network (ANN). Our architecture is composed of a hidden layer, with ten neurons, and a Sigmoid as activation function. The output layer is fully connected to the hidden layer through a single neuron with no bias weights, while the Rectified Linear Unit (ReLU) is taken as activation function to learn the $\beta(t)$ values. The unified ANN architecture and the mathematical model are illustrated in Figure 2. It is important to highlight that our unified methodology falls within the class of hybrid machine learning + SIR-based approaches, as the ANN is combined with a mathematical model of infectious disease to

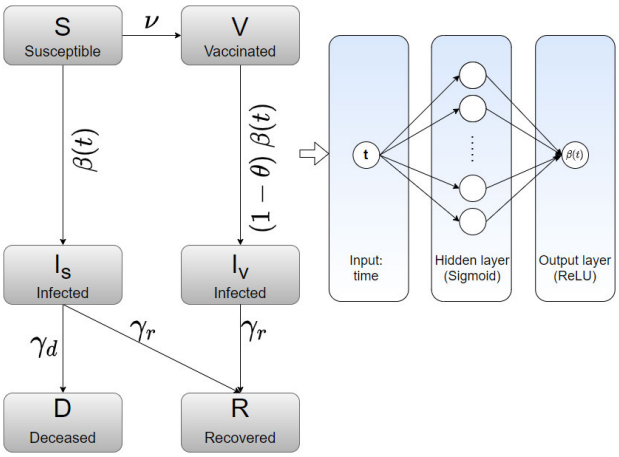

FIGURE 2. Representation of the simplified SVIRD-based framework and the artificial neural network.

estimate the time-dependent parameters used for the computation of epidemiology metrics such as the $R_t(t)$, as well as for COVID-19 time series forecasting. Notice that the advantage of using ANN instead of any other more complex learning design lies in the simplicity and versatility of ANN in successfully learning the unknown parameters of the SVIRD model while still requiring as input only the raw data of infected, recovered, deaths and vaccination to produce the forecasts of epidemiological data, including $R_t(t)$ and vaccinated people with doses 1 and 2.

2) OBTAINING THE MODEL's PARAMETERS

The epidemiological parameters $\beta(t)$, γ_r and γ_d are computed from a learning strategy based on the real data, by minimizing the following loss function:

$$\mathcal{L}(\beta_{\text{net}}(t), \gamma_r, \gamma_d, \nu_1, \nu_2) = \sum_{l \in L} l, \tag{2}$$

where

$$\begin{aligned}
L &= \{l_I, l_R, l_D, l_{v,1}, l_{v,2}, l_{\text{sum}}\},\\
l_I &= \frac{1}{M}\sum_{i=0}^{M}\left|\log(I_i) - \log(\tilde{I}_i)\right|^2,\\
l_R &= \frac{1}{M}\sum_{i=0}^{M}\left|\log(R_i) - \log(\tilde{R}_i)\right|^2,\\
l_D &= \frac{1}{M}\sum_{i=0}^{M}\left|\log(D_i) - \log(\tilde{D}_i)\right|^2,\\
l_{v,1} &= \frac{1}{M}\sum_{i=0}^{M}\left|\log(V_{1,i}) - \log(\tilde{V}_{1,i})\right|^2,\\
l_{v,2} &= \frac{1}{M}\sum_{i=0}^{M}\left|\log(V_{2,i}) - \log(\tilde{V}_{2,i})\right|^2,\\
l_{\text{sum}} &= \frac{1}{M}\sum_{i=0}^{M}\left|\log(\tilde{T}_i)\right|^2,
\end{aligned}$$

$$\begin{aligned}
\tilde{I}_i &= \tilde{I}_s(t_i) + \tilde{I}_{v,1}(t_i) + \tilde{I}_{v,2}(t_i),\\
\tilde{R}_i &= \tilde{R}_s(t_i) + \tilde{R}_{v,1}(t_i) + \tilde{R}_{v,2}(t_i),\\
\tilde{V}_{j,i} &= \tilde{V}_j(t_i) + \tilde{\tilde{V}}_j(t_i) + \tilde{I}_{v,j}(t_i) + \tilde{R}_{v,j}(t_i),\ j = 1, 2,\\
\tilde{T}_i &= \tilde{S}_i + \tilde{I}_i + \tilde{R}_i + \tilde{D}_i + \tilde{V}_{1,i} + \tilde{V}_{2,i}.
\end{aligned}$$

In Equation (2), we make use of the notation X_i and $\tilde{X}_i$ to represent, respectively, the exact and the numerical solutions at the discretized time t_i of a given target variable. Notice that, in the absence of available data of the vaccinated individuals who got infected, we take the number of vaccine shots when computing $l_{v,1}$ and $l_{v,2}$.

In order to assign time variation to the transmission rate, $\beta_{\text{net}}(t)$ is computed from the network-based architecture. As a result, the trainable parameters of the epidemic model are properly learned and computed by solving the following optimization problem:

$$\arg\min_{W,b,\gamma_r,\gamma_d} \mathcal{L}(\beta_{\text{net}}(t), \gamma_r, \gamma_d), \tag{3}$$

where $\{W, b\}$ are the ANN weights and bias.

3) PREDICTING THE ODE VARIABLES

Since we have computed the epidemiological parameters in the previous step, we then apply the numerical solver LSODA for estimating the final forecasts for $t \in [0, M + p]$, where p is the desirable forecast period [10].

4) IMPROVING DATA FITTING CAPABILITY

A moving window-based strategy has been employed to detect and remove data outliers. The rationale is to calibrate the net weights, bias, and parameters γ_r, γ_d, ν_1 and ν_2 for different simulation intervals M_i. This step is accomplished by running Steps (2) and (3) for each M_i, $i = 1, \ldots, n$, where n is a pre-defined value representing the number of windows. In the experiments, we take as time windows 20, by setting the most recent data and taking M_i days before for each running window. For implementation details, see [10].

5) FILTERING OUTLIERS AND GETTING THE FINAL ESTIMATES

For each window, we filter out outliers by comparing the results from Step (3) with the actual data for each target variable. This is performed using the MAPE metric (see Equation (5)). We then determine whether a training window should be discarded or not according to the MAPE calculated. Finally, we compute the geometric mean of the outputs corresponding to the same day to get the final estimate.

B. EFFECTIVE REPRODUCTION NUMBER

Since the effective reproduction number $R_t(t)$ is a very important measure used in infectious diseases, we analyze how the new variables inserted into the mathematical model influence it. Formally speaking, $R_t(t)$ is defined as the quotient between the transmission and recovery rates weighted by the percentage of the susceptible population [10].

FIGURE 3. Geographic location of the investigated regions.

Notice that, in our SVIRD formulation, vaccinated individuals are still susceptible to contagion, but they are subject to a lower rate of infectivity due to the vaccine. Following the multi-group model of the reproduction number given by Driessche and Watmough [37], $R_t(t)$ can be computed as:

$$R_t(t) = \frac{\beta(t)}{\gamma_r}\left[\bar{V}_1 + (1-\theta_1)(V_1 + \bar{V}_2) + (1-\theta_2)V_2\right] + \frac{\beta(t)}{\gamma_r + \gamma_d}S \quad (4)$$

C. DATA SETS AND QUALITY EVALUATION METRICS

The data collection used in our experiments comprises several data resources and public repositories, which vary according to the region/country studied. Below, we detail the data sets employed in our analysis and simulations.

- **Israel dataset**: COVID-19 confirmed cases and deaths data were downloaded from the well-known *Johns Hopkins University* (JHU) data repository [2], which is available at https://coronavirus.jhu.edu/map.html. Concerning vaccination data, it was collected from the *Israel Ministry of Health* website, at https://www.gov.il/en/departments/guides/information-corona.
- **Serrana's town dataset**: Times-series of confirmed cases, recoveries, and deaths data were obtained from the COVID-19 health bulletins of *Serrana's local government*, hosted at http://www.serrana.sp.gov.br/coronavirus. The total number of vaccine doses administered per day was obtained from the *São Paulo State government* website, at https://www.saopaulo.sp.gov.br/planosp/simi/dados-abertos, while the vaccination time-series used to simulate a regular immunization campaign was taken from the online tracking platform *SP Covid-19 Info Tracker* [10], available at http://www.spcovid.net.br.
- **São Paulo State dataset**: Data acquired from the *São Paulo State government* website, including confirmed cases, recoveries, deaths, and the number of immunized people per day for each type of vaccine dose.
- **Brazil dataset**: Time-series taken from the *Brazilian Ministry of Health* website, at https://covid.saude.gov.br. The administered doses per day were obtained from the *Vaccinometer-SUS*, a real-time platform of Brazilian government hosted at https://localizasus.saude.gov.br.

TABLE 2. Efficacy of different vaccine types.

Vaccine	Efficacy Dose 1	Efficacy Dose 2	Efficacy Delay	Source
Coronavac (Sinovac)	$\theta_1 = 5.98\%$	$\theta_2 = 66.48\%$	$\alpha = \frac{1}{14}$	[40]
Pfizer (BioNTech)	$\theta_1 = 52.00\%$	$\theta_2 = 95.00\%$	$\alpha = \frac{1}{21}$	[41]
AstraZeneca (Oxford)	$\theta_1 = 64.00\%$	$\theta_2 = 70.40\%$	$\alpha = \frac{1}{14}$	[42]

The quality of the predictions were assessed via well-established quality evaluation metrics such as *Mean Absolute Percentage Error* (MAPE) [38], [39] and *Normalized Root Mean Square Error* (NRMSE) [10]:

$$\text{MAPE}(Y_i, \tilde{Y}_i) = \frac{1}{n}\sum_{i=1}^{n}\left|\frac{Y_i - \tilde{Y}_i}{Y_i}\right| \times 100, \quad (5)$$

$$\text{NRMSE}(Y_i, \tilde{Y}_i) = \frac{1}{n}\frac{\sqrt{\sum_{i=1}^{n}(Y_i - \tilde{Y}_i)^2}}{\overline{Y}}, \quad (6)$$

where Y_i and $\tilde{Y}_i$ represent the observed and estimated values of a given variable in a time-series of n entries, while $\overline{Y}$ is the average of Y_i.

IV. RESULTS, SIMULATIONS AND DISCUSSION

In this section, we present and discuss the forecast results, simulated scenarios, and the main findings emerging from our data-driven analysis. Parameters θ_1, θ_2 and α used to run the learning steps of the SIR model were taken from the literature, as reported in Table 2. The vaccination rates ν_1 and ν_2 were set according to the total number of vaccinated people per day for each type of vaccine dose as observed in each region/country studied.

A. VALIDATION WITH REAL VACCINATION CAMPAIGNS

In order to assess the proposed methodology, we take as benchmark the well-established vaccination data from Israel, as it has already immunized a large number of people with the Pfizer vaccine [41]. Also, the accuracy of the SIR-based model is attested by analyzing the massive vaccination rollout of Serrana's town: a provincial city of 45,000 inhabitants

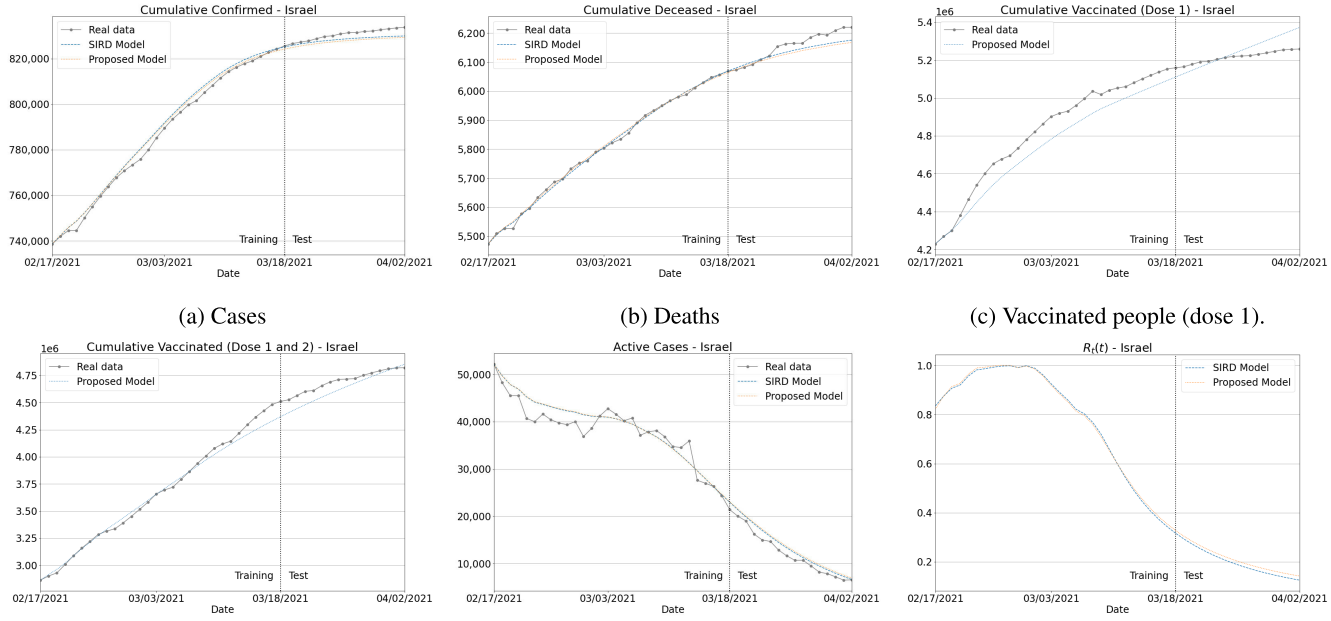

(a) Cases (b) Deaths (c) Vaccinated people (dose 1).

(d) Vaccinated people (doses 1 and 2). (e) Active cases (f) $R_t(t)$

FIGURE 4. **Israel validation results. (a) Confirmed cases, (b) deaths, (c) vaccinated people who received at least one vaccine dose, (d) two doses, (e) active cases, and (f) effective reproduction number. Training period from February 17th 2021 to March 18th 2021.**

located in the State of São Paulo, Brazil. Very recently, Serrana became the first fully immunized city in the world as a result of *Project S* [11], [43], a Brazilian pilot study conducted by the São Paulo State government in cooperation with *Instituto Butantan* [12] designed to address important issues regarding mass vaccination effects of the Coronavac/Sinovac immunizer. Finally, the results obtained from the recently published data-driven model [10] (called here "SIRD") are also presented for the sake of comparison, since it is a robust SIR-based approach that does not include any vaccination dynamics in its formulation.

TABLE 3. **Average MAPE and NRMSE for the two-week forecasting period plotted in Figure 4.**

Variable	Metric	Proposed Model	Data-Driven SIRD
Cases	MAPE	0.370	0.276
	NRMSE	0.004	0.003
Deaths	MAPE	0.467	0.389
	NRMSE	0.006	0.005
Vaccinations (Dose 1)	MAPE	0.888	-
	NRMSE	0.011	-
Vaccinations (Doses 1 and 2)	MAPE	1.476	-
	NRMSE	0.009	-

1) ISRAEL VACCINATION CAMPAIGN

Figure 4 shows the forecasting results, under a 14 days' time horizon, for several Israeli COVID-19 curves. One can verify that our model fits the real scenario as precisely as the SIRD method [10]. However, since the SIRD approach does not take into account a data-driven vaccine compartment, the effects of the transmission rate are only assigned to the learned parameter $\beta(t)$, which attempts to capture the different stages of the virus spreading. On the other hand, our model allows for properly dealing with an immunization campaign, which includes the tuning of the vaccination parameters as well as understanding the role of the vaccinated individuals on the full dynamics of the disease. The reproduction number also follows similar trajectories for both predictors, indicating that active cases and the effective reproduction number $R_t(t)$ significantly decrease when a massive vaccination rollout is combined with a high-efficacy vaccine. Finally, concerning the quantitative verification listed in Table 3, once again both models produce very similar results, as the highest computed MAPE is of the order of less than 1%, i.e., a very small prediction error.

2) SERRANA's TOWN VACCINATION CAMPAIGN

Figure 5 presents the fitting and forecasting results concerning Serrana's massive vaccination campaign. Since the adult residents of Serrana have been immunized with the Sinovac vaccine (Coronavac), we take θ_1 and θ_2 as in Table 2. By visually inspecting the results, both methods follow the trajectories of real data. Moreover, the models have learned the changing trend of active cases, which is reflected by $R_t(t)$ turning less than 1.0 in the second half of March. The vaccination curves were also captured by our approach, even at high immunization rates as those of *Project S* [11]: over 67% of Serrana's adult population had been vaccinated with one shot of Coronavac by March 3rd. Finally, the quality metrics listed in Table 4 indicate a good agreement between the real

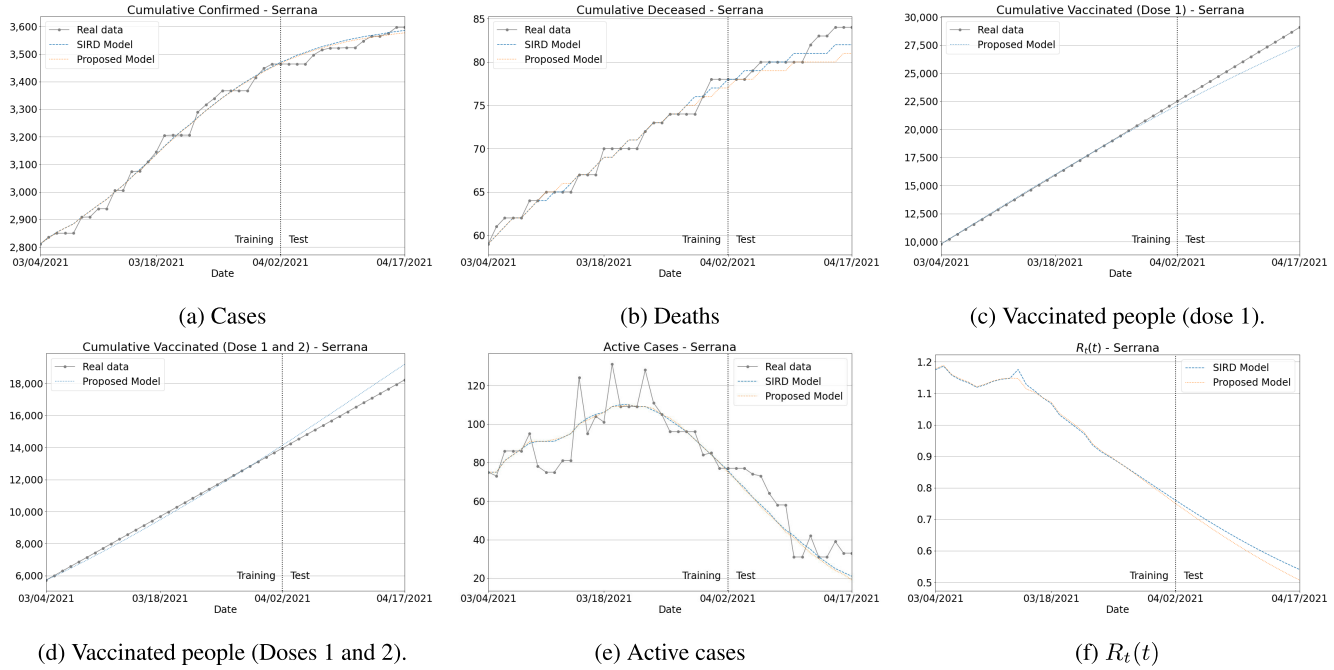

(a) Cases (b) Deaths (c) Vaccinated people (dose 1).

(d) Vaccinated people (Doses 1 and 2). (e) Active cases (f) $R_t(t)$

FIGURE 5. **Serrana's town validation results. (a) Confirmed cases, (b) deaths, (c) vaccinated people who received at least one vaccine dose, (d) two doses, (e) active cases, and (f) effective reproduction number. Training period from March 4th 2021 to April 2nd 2021.**

TABLE 4. **Average MAPE and NRMSE for the two-week forecasting period plotted in Figure 5.**

Variable	Metric	Proposed Model	Data-Driven SIRD
Cases	MAPE	0.449	0.537
	NRMSE	0.005	0.006
Deaths	MAPE	1.733	1.131
	NRMSE	0.023	0.015
Vaccinations (Dose 1)	MAPE	3.520	-
	NRMSE	0.038	-
Vaccinations (Doses 1 and 2)	MAPE	3.404	-
	NRMSE	0.037	-

and the estimated data, as the highest MAPE and NRMSE values are much smaller than 10% and 0.2, respectively.

B. SIMULATION-BASED VACCINATION SCENARIOS

We now assess the impact of different vaccination scenarios for Serrana's town, São Paulo State, and Brazil. More precisely, we simulate a variety of potentially realistic scenarios of vaccinations, by varying in our data-driven technique both the vaccination rates and the immunization efficacies.

1) ASSESSING THE IMPACT OF VACCINATION SPEED AND VACCINE EFFICACY ON A FULLY VACCINATED POPULATION

We start by investigating how the vaccination speed can influence the epidemic curves in a population almost fully immunized as the one in Serrana. For this purpose, we take two evaluation scenarios: (i) the real data from Serrana, including its true vaccination rates as quickly leveraged by *Project S* with the Coronavac vaccine, and (ii) the same data as in (i), but now replacing the Serrana's vaccination rates for another time-series which follows the ''standard'' vaccination rollout as observed in Dracena – another small town in the state of São Paulo about the same size of Serrana. We also simulate the use of several vaccine efficacies according to data reported by the vaccine producers (see Table 2).

The blue and orange lines in Figures 6(a)-(c) give the learned data and future estimates in a time horizon of two-months for scenarios (i) and (ii), respectively. The vaccination speed has positively affected both confirmed cases and deaths. Indeed, after two months, it is expected that the ''orange campaign'' reaches around 140 deaths against 89 for the blue one representing the real immunization program of Serrana. Therefore, the reduction in the total number of COVID-19 fatalities is around 38%, for these two scenarios. Concerning Figure 6(c), immunizing faster reduces $R_t(t)$ by 29% after two months, which is another bonus from accelerated vaccination.

The performance of three vaccine efficacies, Coronavac (blue), AstraZeneca (orange) and Pfizer (green), are displayed in Figures 6(d)-(f). Due to the moderate efficacy of Coronavac, a higher number of cases is observed, while AstraZeneca and Pfizer prevent the virus from spreading more efficiently. At the end of the forecasting interval, the estimates from orange and green lines produce 292 and 306 cases less than the blue one. In contrast to the reduction in the number of cases, deaths avoided by all three immunizers remain at the same level as time advances, thus indicating they are capable of ensuring high protection against COVID-19 mortality. Finally, $R_t(t)$ assigned to

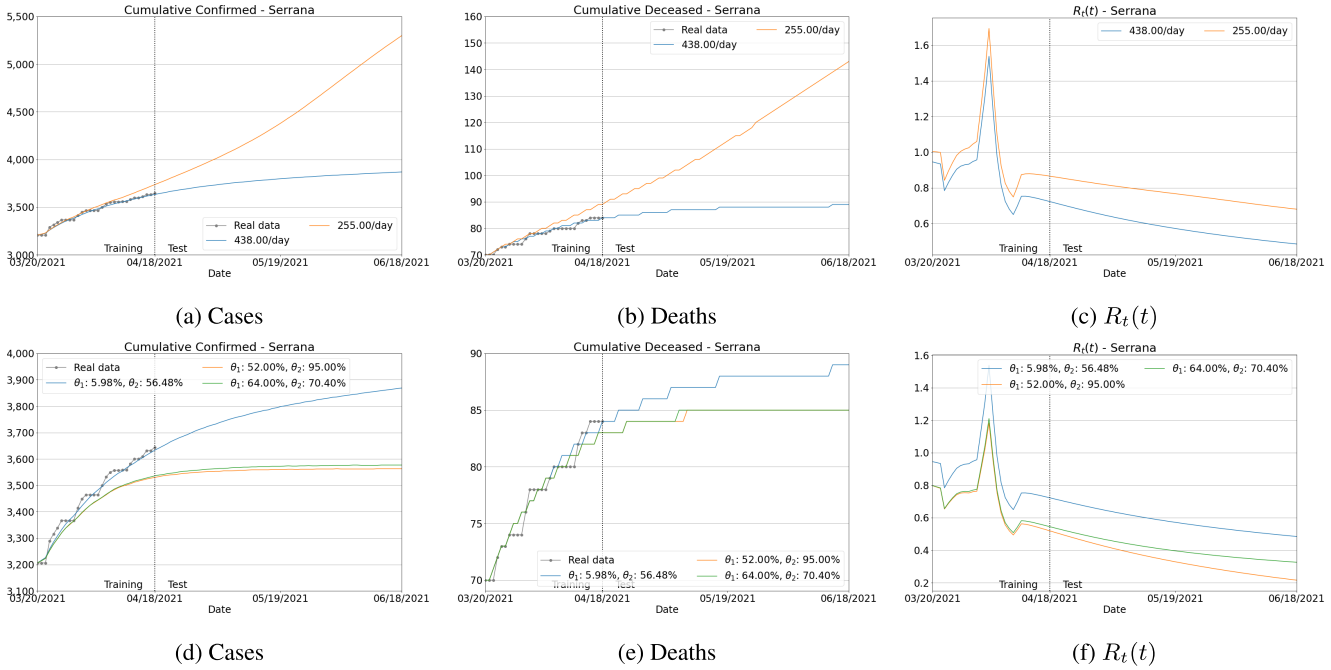

(a) Cases (b) Deaths (c) $R_t(t)$

(d) Cases (e) Deaths (f) $R_t(t)$

FIGURE 6. Serrana's town scenarios results. (a)-(d) Confirmed cases, (b)-(e) deaths, and (c)-(f) effective reproduction number. Training period from March 20th 2021 to April 18th 2021.

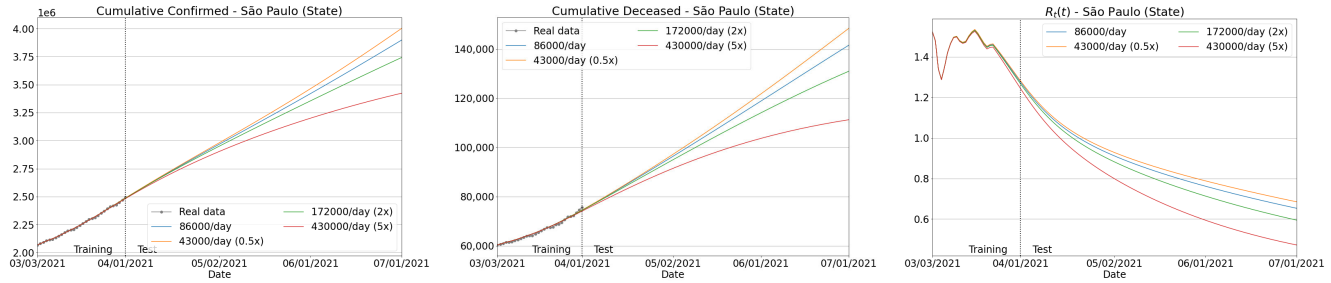

(a) Cases (b) Deaths (c) $R_t(t)$

FIGURE 7. São Paulo state vaccination speed scenarios. (a) Confirmed cases, (b) deaths, and (c) effective reproduction number. Training period from March 3rd 2021 to April 1st 2021.

Coronavac decreases by 31% and 54% when it is compared with AstraZeneca and Pfizer, respectively.

2) ASSESSING THE IMPACT OF VACCINATION SPEED ON A PARTIALLY IMMUNIZED POPULATION

We now evaluate the impact of different immunization rates in a much bigger population: São Paulo State, which is the most populous state in Brazil, home to around 46 million people, i.e., the same as Spain. Notice that the vaccination rollout in São Paulo is still in progress so that the percentage of vaccinated people with at least one vaccine dose reached 20% only recently. To design this experiment, in Figure 7 we take the real data from March 3rd to April 1nd, to train the model, and then simulate the next three months of the pandemic. Four vaccination speed rates were simulated: the blue one is the real data, and then rates are set to 0.5x (orange), 2x (green), and 5x (red). Confirmed cases decrease slowly as the vaccination advances, except for the real speed against the 5x campaign: the cases drop from around 3.9 to 3.4 million, a reduction of 13%. Similarly, deaths are substantially mitigated as more people are vaccinated in an increasingly short period, dropping from 141,000 (blue) to 131,000 (green) and 111,000 (red). Finally, by accelerating the vaccination, the transmission rate is also pulled down. Thus, this experiment confirms how important it is to speed up vaccination, as done in Israel, UK, and USA.

3) ASSESSING THE IMPACT OF DIFFERENT COVID-19 VACCINES

Figure 8 displays how vaccine efficacies can influence the infectivity of SARS-CoV-2 in São Paulo and Brazil. Together with Coronavac (purple), AstraZeneca (red) and

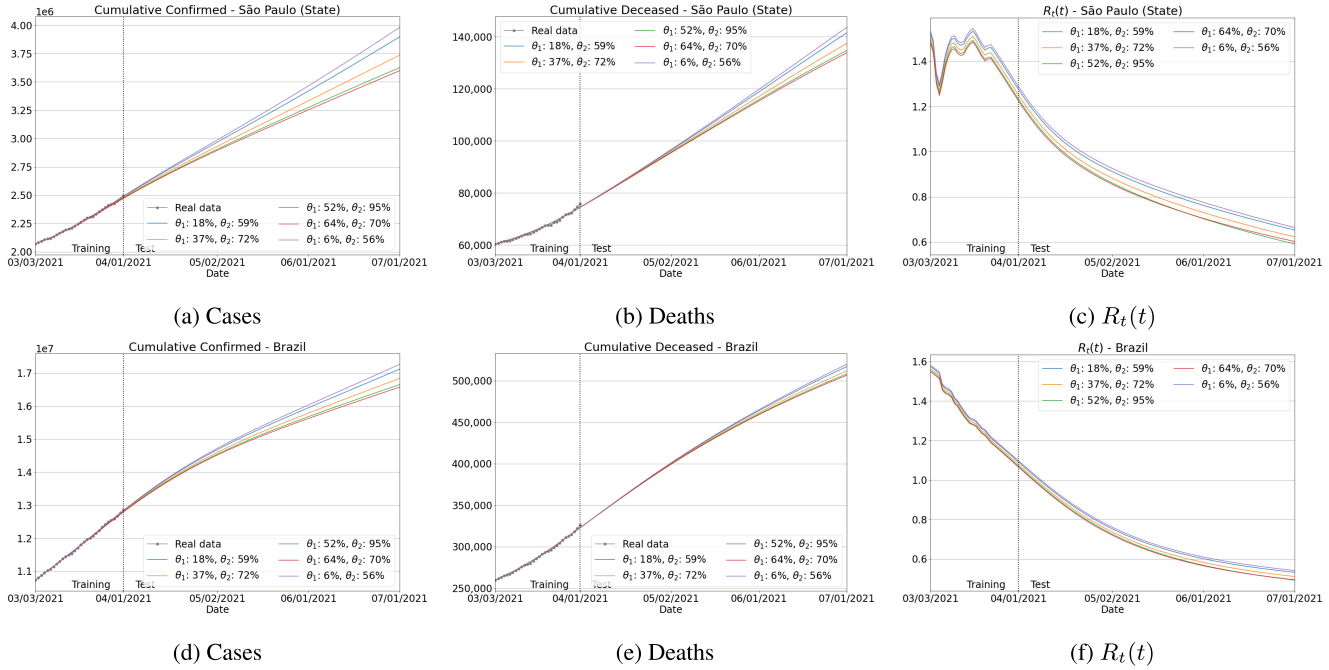

(a) Cases (b) Deaths (c) $R_t(t)$

(d) Cases (e) Deaths (f) $R_t(t)$

FIGURE 8. São Paulo state and Brazil COVID-19 vaccines scenarios. (a)-(d) Confirmed cases, (b)-(e) deaths, and (c)-(f) effective reproduction number. Training period from March 3rd 2021 to April 1st 2021.

TABLE 5. Mixed vaccine proportions and their resulting efficacies used to run the experiments in Figures 8 and 9. Brazilian vaccine distribution (in blue) taken from *Ministry of Health - Brazil* [44] on March 31, 2021.

Coronavac	AstraZeneca	Pfizer	Resulting Efficacy	Color
80%	20%	0%	$\theta_1 = 18\%$ $\theta_2 = 59\%$	blue
40%	30%	30%	$\theta_1 = 37\%$ $\theta_2 = 72\%$	orange
100%	0%	0%	$\theta_1 = 6\%$ $\theta_2 = 56\%$	purple
0%	100%	0%	$\theta_1 = 64\%$ $\theta_2 = 70\%$	red
0%	0%	100%	$\theta_1 = 52\%$ $\theta_2 = 95\%$	green

TABLE 6. Vaccine efficacy comparison from the current scenario ($\theta_1 = 18\%$, $\theta_2 = 59\%$ - Blue line from Figure 8).

Efficacy	Cases		Deaths	
	São Paulo	Brazil	São Paulo	Brazil
Baseline	1,395,106	4,217,642	66,339	191,676
$\theta_1 = 37\%$ $\theta_2 = 72\%$ (Orange)	1,241,105 (-11.0%)	3,955,485 (-6.2%)	62,326 (-6.0%)	186,396 (-2.8%)
$\theta_1 = 52\%$ $\theta_2 = 95\%$ (Green)	1,137,064 (-18.5%)	3,783,811 (-10.3%)	59,605 (-10.2%)	182,920 (-4.6%)
$\theta_1 = 64\%$ $\theta_2 = 70\%$ (Red)	1,113,243 (-20.2%)	3,713,921 (-11.9%)	58,743 (-11.5%)	181,273 (-5.4%)
$\theta_1 = 6\%$ $\theta_2 = 56\%$ (Purple)	1,474,225 (+5.7%)	4,353,357 (+3.2%)	68,407 (+3.1%)	194,424 (+1.4%)

Pfizer (green) efficacies, we take two combinations of mixed efficacies (blue and orange), to simulate the vaccination roll-outs with multiple types of vaccines in São Paulo and Brazil. Table 5 lists several combinations of vaccines, by computing the weighted average between their real efficacies and the number of administrated doses.

First, considering São Paulo's case study, efficacies related to AstraZeneca, Pfizer, and the combination $\theta_1 = 37\%$ with $\theta_2 = 72\%$ make the confirmed cases to go down more quickly compared to the purple and blue curves. Indeed, green and red campaigns perform similarly, producing the lowest number of cases, i.e., 362k and 360k against 398k from Coronavac. Moreover, the first dose efficacy plays a key role in the immunization process. Deaths are also mitigated when taking vaccines of greater efficacy. For example, a campaign purely based on Coronavac vaccine reaches around $1.43K$ deaths at the end of the period against $1.34k$ and $1.33k$ deaths from campaigns with Pfizer and AstraZeneca. A similar pandemic signature is observed in Brazil: if one assumes the current scenario (blue line), from Figure 8 and Table 6, the highest reduction of cases and deaths are delivered by the AstraZeneca vaccine with the current immunization speed, and with Pfizer when boosting 5x the vaccination speed. Finally, $R_t(t)$ drops significantly more than 50% if the speed is increased by 5x with $\theta_1 = 52\%$ and $\theta_2 = 95\%$.

4) ASSESSING THE IMPACT ON INCREASING THE VACCINATION SPEED AS THE VACCINE EFFICACY CHANGES

Next, we evaluate the combined impact of accelerating the vaccination speed as θ_1 and θ_2 vary. To design this

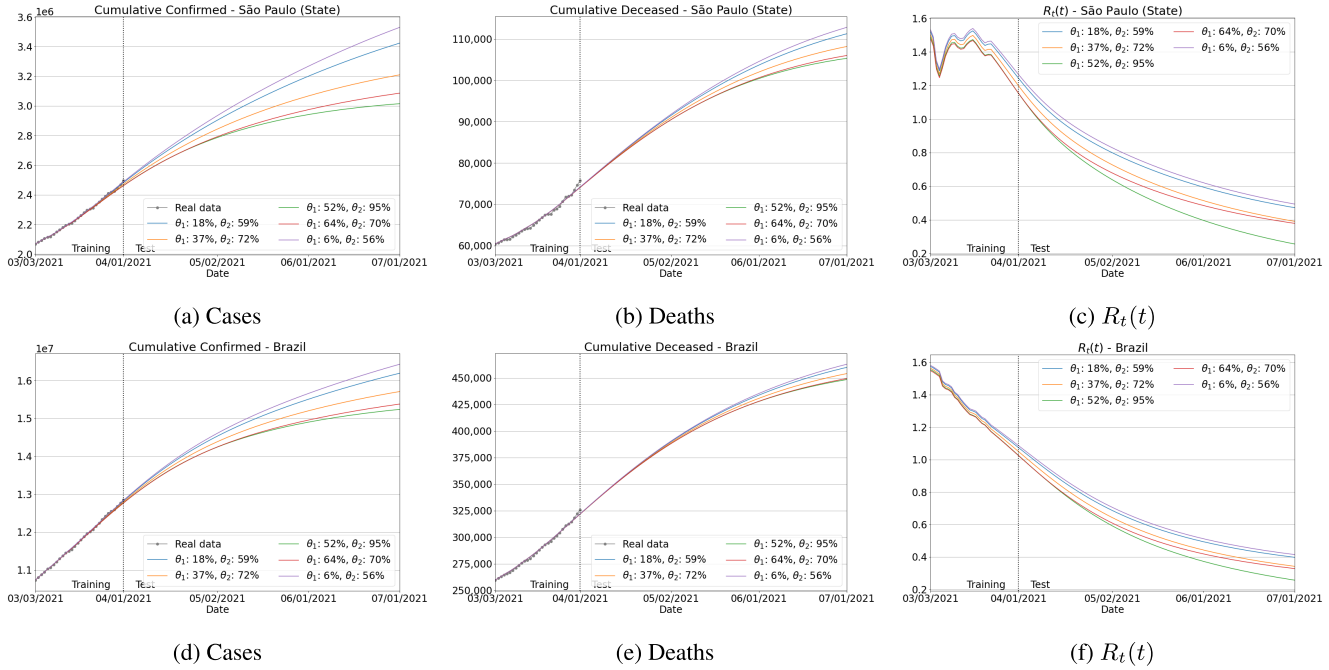

(a) Cases (b) Deaths (c) $R_t(t)$

(d) Cases (e) Deaths (f) $R_t(t)$

FIGURE 9. São Paulo state and Brazil COVID-19 vaccines and vaccination speed scenarios. (a)-(d) Confirmed cases, (b)-(e) deaths, and (c)-(f) effective reproduction number. Training period from March 3rd 2021 to April 1st 2021.

TABLE 7. Vaccine efficacy comparison by taking as baseline the blue line from Figure 9.

Efficacy	Cases		Deaths	
	São Paulo	Brazil	São Paulo	Brazil
Baseline	925,808	3,303,194	36,511	135,479
$\theta_1 = 37\%$ $\theta_2 = 72\%$ (Orange)	722,785 (-21.9%)	2,848,722 (-13.8%)	33,476 (-8.3%)	129,701 (-4.3%)
$\theta_1 = 52\%$ $\theta_2 = 95\%$ (Green)	538,536 (-41.8%)	2,404,922 (-27.2%)	30,648 (-16.1%)	124,115 (-8.4%)
$\theta_1 = 64\%$ $\theta_2 = 70\%$ (Red)	610,734 (-34.0%)	2,549,897 (-22.8%)	31,348 (-14.1%)	125,126 (-7.6%)
$\theta_1 = 6\%$ $\theta_2 = 56\%$ (Purple)	1,026,201 (+10.8%)	3,524,649 (+6.7%)	38,043 (+4.2%)	138,380 (+2.1%)

TABLE 8. Vaccine efficacy comparison by taking as baseline the current scenarios in São Paulo and Brazil.

Efficacy	Cases		Deaths	
	São Paulo	Brazil	São Paulo	Brazil
Baseline	1,395,106	4,217,642	66,339	191,676
$\theta_1 = 18\%$ $\theta_2 = 59\%$ (Blue)	925,808 (-33.6%)	3,303,194 (-21.7%)	36,511 (-45.0%)	135,479 (-29.3%)
$\theta_1 = 37\%$ $\theta_2 = 72\%$ (Orange)	722,785 (-48.2%)	2,848,722 (-32.5%)	33,476 (-49.5%)	129,701 (-32.3%)
$\theta_1 = 52\%$ $\theta_2 = 95\%$ (Green)	538,536 (-61.4%)	2,404,922 (-43.0%)	30,648 (-53.8%)	124,115 (-35.2%)
$\theta_1 = 64\%$ $\theta_2 = 70\%$ (Red)	610,734 (-56.2%)	2,549,897 (-39.5%)	31,348 (-52.7%)	125,126 (-34.7%)
$\theta_1 = 6\%$ $\theta_2 = 56\%$ (Purple)	1,026,201 (-26.4%)	3,524,649 (-16.4%)	38,043 (-42.7%)	138,380 (-27.8%)

experiment, we assume in Figure 9 that the vaccination advances 5x faster than the real immunization campaign in São Paulo and Brazil. In contrast to the results from the current vaccination rates, as previously discussed in Figures 6 and 8, all the vaccines in Figure 9 and Table 7 significantly contribute to the flattening of the curves, making the gaps between them much more prominent with the increased vaccination. Also, from Table 7, one can check that the reduction in cases and $R_t(t)$ are more pronounced than deaths, as expected, given the COVID-19 vaccines are highly effective against deaths.

Finally, in Table 8, we discuss the reduction of COVID-19 rates in São Paulo and Brazil for a three-month forecasting period with their actual immunization campaigns against the hypothetical scenarios with the vaccination speed increased by 5x. From the tabulated results, notice that the total number of cases and deaths are significantly attenuated as more people are vaccinated over the period considered. In fact, even though the most significant falls in confirmed cases have been found with the Pfizer vaccine, all immunizers clearly reduce deaths to similar levels, especially in Brazil (see the last column in Table 8).

V. LIMITATIONS OF THE STUDY

Despite the good properties and results, there are two aspects to be observed when using our methodology. First, the more accurate the data source used, the better the model's assertiveness. For instance, the excessive delay in publicly reporting

COVID-19 cases by Brazilian Government sources may negatively impact the training step of our approach due to the large peaks artificially created in the collected data.

Another issue is related to the vaccine efficacies took to perform the simulations. Although we have adopted the efficacies as reported in the pioneering studies conducted by the vaccine producers, other more recent works have also investigated the efficacy of the doses under different populations and immunization circumstances. However, new vaccination scenarios could be easily built just by re-setting new vaccine efficacies into the dynamic SVIRD model.

VI. CONCLUSION

In this work, we provided several simulation-based evaluations of the pros and cons of COVID-19 vaccination campaigns in Brazil, São Paulo State, and Serrana's town. Our analysis concentrated on assessing the impacts of the immunization speed and vaccine efficacy in the epidemic curves of confirmed cases, deaths and infectivity rate, for at least three types of immunizers. The study was conducted by applying a SIR-based model combined with a Machine Learning strategy, yielding a new data-driven methodology used to fit the epidemic curves as well as to predict the behavior and trends of the time-series.

As discussed in Section IV, the use of different vaccines indicates that, between them, the difference in confirmed cases is more pronounced than in the deceased. In fact, we found that the protection against SARS-CoV-2 deaths is similar among all immunizers, in line with published clinical studies. Another finding is that the speed in administering new shots of vaccine is of paramount importance to pull down the deaths and infectivity levels of the disease, even for those COVID-19 immunizers with moderate efficacy. For example, we have found that confirmed cases and deaths in Brazil may be pruned to around 16% and 27%, by adopting an immunization campaign purely carried out with a vaccine of moderate efficacy as long as the speed of vaccination is accelerated.

Finally, as shown in Figure 8 and 9, our methodology can be successfully used to perform numerical investigation concerning the recent strategy of mix-and-match vaccination, as the one in progress in the UK according to the Com-COV Study Team [13].

REFERENCES

[1] H. Ritchie, E. Mathieu, L. Rodés-Guirao, C. Appel, C. Giattino, E. Ortiz-Ospina, J. Hasell, B. Macdonald, D. Beltekian, and M. Roser, "Coronavirus pandemic (COVID-19)," *Our World in Data*, Mar. 2020. [Online]. Available: http://www.ourworldindata.org/coronavirus

[2] E. Dong, H. Du, and L. Gardner, "An interactive web-based dashboard to track COVID-19 in real time," *Lancet Infectious Diseases*, vol. 20, no. 5, pp. 533–534, 2020.

[3] Johns Hopkins University. (2020). *COVID-19 Data Repository by the Center for Systems Science and Engineering (CSSE) at Johns Hopkins University*. [Online]. Available: https://github.com/CSSEGISandData/COVID-19

[4] The New York Times. (2021). *Bolsonaro Talked Vaccines Down. Now Brazil Has Too Few Doses*. [Online]. Available: https://www.nytimes.com/2021/01/18/world/americas/brazil-covid-variants-vaccinations.html

[5] C. C. D. S. A. Matos, C. L. A. Barbieri, and M. T. Couto, "Covid-19 and its impact on immunization programs: Reflections from Brazil," *Revista de Saúde Pública*, vol. 54, p. 114, Dec. 2020.

[6] R. Castro. (Mar. 2021). *COVID-19 Observatory Points to the Biggest Health System Collapse in the History of Brazil*. [Online]. Available: https://portal.fiocruz.br/en/news/covid-19-observatory-points-biggest-health-system-collapse-history-brazil

[7] R. M. Coutinho, F. M. D. Marquitti, L. S. Ferreira, M. E. Borges, R. L. P. da Silva, O. Canton, T. P. Portella, S. P. Lyra, C. Franco, A. A. M. da Silva, R. A. Kraenkel, M. A. D. S. M. Veras, and P. I. Prado, "Model-based evaluation of transmissibility and reinfection for the P. 1 variant of the SARS-CoV-2," *medRxiv*, Mar. 2021.

[8] E. V. M. dos Reis and M. A. Savi, "A dynamical map to describe COVID-19 epidemics," *medRxiv*, Aug. 2021.

[9] M. Amaku, D. T. Covas, F. A. B. Coutinho, R. S. Azevedo, and E. Massad, "Modelling the impact of delaying vaccination against SARS-CoV-2 assuming unlimited vaccine supply," *Theor. Biol. Med. Model.*, vol. 18, no. 1, p. 14, Dec. 2021.

[10] F. Amaral, W. Casaca, C. M. Oishi, and J. A. Cuminato, "Towards providing effective data-driven responses to predict the Covid-19 in São Paulo and Brazil," *Sensors*, vol. 21, no. 2, p. 540, Jan. 2021.

[11] The Telegraph. (2021). *Project S: Entire Town Vaccinated as Experts Race to Understand if COVID Jabs Halt Transmission*. [Online]. Available: https://www.telegraph.co.uk/global-health/science-and-disease/project-s-entire-town-vaccinated-experts-race-understand-covid/

[12] Instituto Butantan. (2021). *Instituto Butantan*. [Online]. Available: https://butantan.gov.br/instituto-butantan/about-us

[13] R. H. Shaw, A. Stuart, M. Greenland, X. Liu, J. S. N. Van-Tam, and M. D. Snape, "Heterologous prime-boost COVID-19 vaccination: Initial reactogenicity data," *Lancet*, vol. 397, no. 10289, pp. 2043–2046, May 2021, doi: 10.1016/S0140-6736(21)01115-6.

[14] E. Callaway. (May 2021). *Mix-and-Match COVID Vaccines Trigger Potent Immune Response*. [Online]. Available: https://www.nature.com/articles/d41586-021-01359-3

[15] M. E. Alexander, C. Bowman, S. M. Moghadas, R. Summers, A. B. Gumel, and B. M. Sahai, "A vaccination model for transmission dynamics of influenza," *SIAM J. Appl. Dyn. Syst.*, vol. 3, no. 4, pp. 503–524, Jan. 2004.

[16] M. J. Counotte, C. L. Althaus, N. Low, and J. Riou, "Impact of age-specific immunity on the timing and burden of the next Zika virus outbreak," *PLOS Neglected Tropical Diseases*, vol. 13, no. 12, Dec. 2019, Art. no. e0007978.

[17] C. Sun and Y.-H. Hsieh, "Global analysis of an SEIR model with varying population size and vaccination," *Appl. Math. Model.*, vol. 34, no. 10, pp. 2685–2697, Oct. 2010.

[18] S. Sinha, O. Misra, and J. Dhar, "Stability analysis of sir model with vaccination," *Amer. J. Comput. Appl. Math.*, vol. 4, pp. 17–23, Jan. 2014.

[19] K. S. Mathur and P. Narayan, "Dynamics of an *SVEIRS* epidemic model with vaccination and saturated incidence rate," *Int. J. Appl. Comput. Math.*, vol. 4, no. 5, p. 118, Oct. 2018.

[20] S. Roy, R. Dutta, and P. Ghosh, "Optimal time-varying vaccine allocation amid pandemics with uncertain immunity ratios," *IEEE Access*, vol. 9, pp. 15110–15121, 2021.

[21] M. Fudolig and R. Howard, "The local stability of a modified multi-strain sir model for emerging viral strains," *PLoS ONE*, vol. 15, no. 12, pp. 1–27, Dec. 2020.

[22] C. M. Saad-Roy, S. E. Morris, C. J. E. Metcalf, M. J. Mina, R. E. Baker, J. Farrar, E. C. Holmes, O. G. Pybus, A. L. Graham, S. A. Levin, B. T. Grenfell, and C. E. Wagner, "Epidemiological and evolutionary considerations of SARS-CoV-2 vaccine dosing regimes," *Science*, vol. 372, no. 6540, pp. 363–370, Apr. 2021.

[23] S. Berkane, I. Harizi, and A. Tayebi, "Modeling the effect of population-wide vaccination on the evolution of COVID-19 epidemic in Canada," *medRxiv*, Apr. 2021.

[24] M. Etxeberria-Etxaniz, S. Alonso-Quesada, and M. De la Sen, "On an SEIR epidemic model with vaccination of newborns and periodic impulsive vaccination with eventual on-line adapted vaccination strategies to the varying levels of the susceptible subpopulation," *Appl. Sci.*, vol. 10, no. 22, p. 8296, Nov. 2020.

[25] N. P. Rachaniotis, T. K. Dasaklis, F. Fotopoulos, and P. Tinios, "A two-phase stochastic dynamic model for COVID-19 mid-term policy recommendations in greece: A pathway towards mass vaccination," *Int. J. Environ. Res. Public Health*, vol. 18, no. 5, p. 2497, Mar. 2021.

[26] M. De la Sen, S. Alonso-Quesada, and A. Ibeas, "On a discrete SEIR epidemic model with exposed infectivity, feedback vaccination and partial delayed re-susceptibility," *Mathematics*, vol. 9, no. 5, p. 520, Mar. 2021.

[27] H.-Y. Mak, T. Dai, and C. S. Tang, "Managing two-dose COVID-19 vaccine rollouts with limited supply," *SSRN Electron. J.*, Feb. 2021.
[28] K. N. Nabi, M. T. Tahmid, A. Rafi, M. E. Kader, and M. A. Haider, "Forecasting COVID-19 cases: A comparative analysis between recurrent and convolutional neural networks," *Results Phys.*, vol. 24, May 2021, Art. no. 104137.
[29] F. Liu, J. Wang, J. Liu, Y. Li, D. Liu, J. Tong, Z. Li, D. Yu, Y. Fan, X. Bi, X. Zhang, and S. Mo, "Predicting and analyzing the COVID-19 epidemic in China: Based on SEIRD, LSTM and GWR models," *PLoS ONE*, vol. 15, no. 8, pp. 1–22, Aug. 2020, doi: 10.1371/journal.pone.0238280.
[30] K. E. ArunKumar, D. V. Kalaga, C. M. S. Kumar, M. Kawaji, and T. M. Brenza, "Forecasting of COVID-19 using deep layer recurrent neural networks (RNNs) with gated recurrent units (GRUs) and long short-term memory (LSTM) cells," *Chaos, Solitons Fractals*, vol. 146, May 2021, Art. no. 110861.
[31] S. Shastri, K. Singh, S. Kumar, P. Kour, and V. Mansotra, "Time series forecasting of COVID-19 using deep learning models: India-USA comparative case study," *Chaos, Solitons Fractals*, vol. 140, Nov. 2020, Art. no. 110227.
[32] G. Spadon, S. Hong, B. Brandoli, S. Matwin, J. F. Rodrigues, Jr., and J. Sun, "Pay attention to evolution: Time series forecasting with deep graph-evolution learning," *IEEE Trans. Pattern Anal. Mach. Intell.*, early access, Apr. 27, 2021, doi: 10.1109/TPAMI.2021.3076155.
[33] L. Mohimont, A. Chemchem, F. Alin, M. Krajecki, and L. A. Steffenel, "Convolutional neural networks and temporal CNNs for COVID-19 forecasting in France," *Appl. Intell.*, vol. 52, pp. 1–26, Apr. 2021.
[34] J. Frausto-Solís, L. J. Hernández-González, J. J. González-Barbosa, J. P. Sánchez-Hernández, and E. Román-Rangel, "Convolutional neural Network–Component transformation (CNN–CT) for confirmed COVID-19 cases," *Math. Comput. Appl.*, vol. 26, no. 2, p. 29, Apr. 2021.
[35] F. Baldo, L. Dall'Olio, M. Ceccarelli, R. Scheda, M. Lombardi, A. Borghesi, S. Diciotti, and M. Milano, "Deep learning for virus-spreading forecasting: A brief survey," 2021, *arXiv:2103.02346*. [Online]. Available: https://arxiv.org/abs/2103.02346
[36] M. Kim, "Prediction of COVID-19 confirmed cases after vaccination: Based on statistical and deep learning models," *SciMedicine J.*, vol. 3, no. 2, pp. 153–165, Jun. 2021.
[37] P. van den Driessche and J. Watmough, "Reproduction numbers and sub-threshold endemic equilibria for compartmental models of disease transmission," *Math. Biosci.*, vol. 180, no. 12, pp. 29–48, Nov./Dec. 2002.
[38] J. V. Leme, W. Casaca, M. Colnago, and M. A. Dias, "Towards assessing the electricity demand in Brazil: Data-driven analysis and ensemble learning models," *Energies*, vol. 13, no. 6, p. 1407, Mar. 2020.
[39] O. Istaiteh, T. Owais, N. Al-Madi, and S. Abu-Soud, "Machine learning approaches for COVID-19 forecasting," in *Proc. Int. Conf. Intell. Data Sci. Technol. Appl. (IDSTA)*, Oct. 2020, pp. 50–57.
[40] (2021). *Strategic Advisory Group of Experts (SAGE) Working Group on COVID-19 Vaccine. Evidence Assessment: Coronavac COVID-19 Vaccine*. [Online]. Available: https://cdn.who.int/media/docs/default-source/immunization/sage/2021/april/5_sage29apr2021_critical-evidence_sinovac.pdf
[41] F. P. Polack, S. J. Thomas, N. Kitchin, J. Absalon, A. Gurtman, S. Lockhart, J. L. Perez, G. P. Marc, E. D. Moreira, C. Zerbini, and R. Bailey, "Safety and efficacy of the BNT162b2 mRNA Covid-19 vaccine," *New England J. Med.*, vol. 383, no. 27, pp. 2603–2615, 2020.
[42] M. Voysey, S. A. C. Clemens, S. A. Madhi, L. Y. Weckx, P. M. Folegatti, P. K. Aley, B. Angus, V. L. Baillie, S. L. Barnabas, Q. E. Bhorat, and S. Bibi, "Safety and efficacy of the ChAdOx1 nCoV-19 vaccine (AZD1222) against SARS-CoV-2: An interim analysis of four randomised controlled trials in Brazil, South Africa, and the UK," *Lancet*, vol. 397, no. 10269, pp. 99–111, 2021.
[43] Reuters. (2021). *As COVID Explodes in Brazil, Serrana Becomes World's First Fully Vaccinated City*. [Online]. Available: https://worldcrunch.com/coronavirus/as-covid-explodes-in-brazil-serrana-becomes-world39s-first-fully-vaccinated-city
[44] Ministry of Health (Brazil). (2021). *COVID-19 Vaccination: Applied Doses Dashboard*. [Online]. Available: https://qsprod.saude.gov.br/extensions/DEMAS_C19Vacina/DEMAS_C19Vacina.html

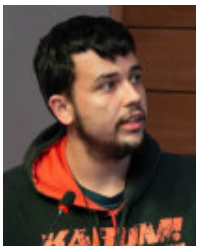

FABIO AMARAL received the B.Sc. degree in computer science and the master's degree in computational mathematics from the Faculty of Science and Technology (FCT), São Paulo State University (UNESP), where he is currently pursuing the Ph.D. degree in computer science. He conducts research on computational intelligence focused on differential equations and numerical-based strategies at UNESP.

WALLACE CASACA received the B.Sc. and master's degrees in pure and applied mathematics from São Paulo State University (UNESP), Brazil, in 2008 and 2010, respectively, and the Ph.D. degree in computer science and applied mathematics from the ICMC, University of São Paulo (USP), Brazil, in 2014. As part of his Ph.D. studies, he worked as a Visiting Researcher with the School of Engineering, Brown University, Providence, RI, USA. He is currently working as an Associate Professor of computer science and mathematics with UNESP/Rosana. His research interests include data science, computer vision, remote sensing, information visualization, optimization, partial differential equations, and numerical analysis.

CASSIO M. OISHI is currently an Associate Professor with the Faculdade de Ciências e Tecnologia (FCT), São Paulo State University (UNESP), Presidente Prudente, Brazil. He is also a Principal Investigator with the Center for Research in Mathematical Sciences Applied to Industry (CeMEAI-FAPESP), a council formed by the main universities at São Paulo state. He is a Research Fellow of the Brazilian National Research Council (CNPq). His Ph.D. thesis on computational mathematics was concluded at the ICMC, University of São Paulo (USP), in August 2008. His research interests include numerical solutions of partial differential equations, data science, computational methodologies for treating moving interface problems, and the development of codes for non-Newtonian fluid mechanics.

JOSÉ A. CUMINATO received the Ph.D. degree in numerical analysis from Oxford University, in 1987. He is currently the Head of the Center for Research in Mathematical Sciences Applied to Industry (CeMEAI-FAPESP). His research interests include simulations of incompressible flows and free surface flows, and finite difference methods, numerical methods for ordinary and partial differential equations, and integral equations of Fredholm and Cauchy. He is a member of the Brazilian Academy of Science and a Corresponding Fellow for the Royal Society of Edinburgh (FRSE). From 2005 to 2007 and from 2007 to 2009, he was the President of the Brazilian Society of Computational and Applied Mathematics, for two terms.